LWT - Food Science and Technology 93 (2018) 329–338

Contents lists available at ScienceDirect

LWT - Food Science and Technology

journal homepage: www.elsevier.com/locate/lwt

Compression molded LLDPE films loaded with bimetallic (Ag-Cu) nanoparticles and cinnamon essential oil for chicken meat packaging applications

Jasim Ahmed[a,*], Mehrajfatemah Mulla[a], Yasir Ali Arfat[a], Anibal Bher[b,c,d], Harsha Jacob[a], Rafael Auras[b]

[a] Food and Nutrition Program, Environment & Life Sciences Research Center, Kuwait Institute for Scientific Research, P.O. Box 24885, Safat 13109, Kuwait
[b] School of Packaging, Michigan State University, East Lansing, MI, 48824-1223, United States
[c] Instituto Sabato, UNSAM-CNEA, San Martin, Buenos Aires, Argentina
[d] Instituto de Materiales de Misiones (IMAM), CONICET-UNaM, Posadas, Misiones, Argentina

ARTICLE INFO

Keywords:
LLDPE
Ag-Cu nanocomposite
Essential oil
Active packaging
Chicken meat

ABSTRACT

This study describes the development of bioactive linear low-density polyethylene (LLDPE) films, blended with cinnamon essential oil (CEO), and selected concentrations of silver-copper (Ag-Cu) nanoparticles (NPs), and processed by compression molding. Influence of Ag-Cu NPs and CEO on thermo-rheological, structural, barrier, morphological and antimicrobial properties of LLDPE composite films were investigated. Ag-Cu NPs reinforcement effectively improved the mechanical and barrier properties of the films, whereas, CEO improved the flexibility of the composite films by lowering the complex viscosity and the melting temperature. The composite films exhibited excellent anti-UV properties, and appearance of new peaks corresponding to the aromatic domain with N-H bending vibration was confirmed by FTIR spectroscopy. Films loaded with Ag-Cu NPs and 50% CEO showed maximum antimicrobial activity against *Listeria monocytogenes, Salmonella* Typhimurium and *Campylobacter jejuni.* Chicken samples contaminated with *S.* Typhimurium and *C. jejuni;* packed in the composite films containing 4% (w/w) Ag-Cu and 50% CEO (w/w), and stored at refrigerated temperature for 21 days showed a complete inhibition.

1. Introduction

Outbreaks of foodborne illnesses are a public health concern. Foodborne diseases annually cause as many as 600 million illnesses and 420,000 deaths worldwide (WHO, 2015). *Salmonella* spp., *Campylobacter* spp. and *Listeria* spp. are among the top pathogens causing foodborne diseases (Trimoulinard et al., 2017); the most important risk factors responsible for the infection have included the handling and consumption of raw or undercooked chicken or other meats, raw milk and surface waters (EFSA, 2009). Active packaging (AP) is one of the novel food packaging concepts that have been presented as a response to the consumers' demand for minimally processed and preservative-free products. In AP, microbes are constantly controlled by the release of active compounds embedded in the packaging materials during transportation and storage. Polyethylene (PE) is one of the commercially used polyolefins and accounts for more than 70% of the plastics in the market because of its abundant supply, good chemical resistance, high impact strength, and a low cost (Berger et al., 2017). Polyolefins find a wide range of applications in packaging including film productions, injection molding, and compression molding. In comparison to other PEs, linear low-density polyethylene (LLDPE) provides better processability, lower manufacturing costs, and improved mechanical properties such as toughness for the packaging applications; however, it also has some limitations such as poor oxygen and UV barrier properties (Villaluenga & Seoane, 1998). In response to those limitations, polymer nanocomposites have been developed for both packaging and engineering applications with the desirable thermo-mechanical and barrier properties.

Metal or metal oxide NPs (gold, silver, zinc, and copper) have been employed as reinforcing fillers in polymer matrices to improve their functional, mechanical, antimicrobial, and barrier properties (Raquez, Habibi, Murariu, & Dubois, 2013). Alloyed bimetallic NPs including Ag-Cu alloy NPs exhibited improved antibacterial activity even in small quantities over individual Ag or Cu NPs (Zain, Stapley, & Shama, 2014). Additionally, these NPs are approved by the United States Food and Drug Administration (FDA) for use in food packaging materials (FDA,

* Corresponding author.
E-mail addresses: jaahmed@kisr.edu.kw, jahmed2k@yahoo.com (J. Ahmed).

https://doi.org/10.1016/j.lwt.2018.03.051
Received 19 October 2017; Received in revised form 16 March 2018; Accepted 19 March 2018
Available online 21 March 2018
0023-6438/

2015). However, the loading of bimetallic NPs like Ag-Cu into LLDPE polymer matrix and properties of resulting nanocomposites have not yet been reported.

Combination of various antimicrobials seems to be the best strategy for controlling the resistant bacterial cells (Scandorieiro et al., 2016), and therefore, a combination of NPs with naturally derived essential oils (EOs) could be the best selection for the inactivation of pathogens. Plant extracts such as cinnamon essential oil (CEO) have shown higher activity against *E. coli, L. monocytogenes*, yeast, and molds (Rodriguez, Batlle, & Nerin, 2007). In our previous work, we observed that a higher microbial reduction of *L. monocytogenes and S.* Typhimurium were achieved when 50% CEO was incorporated into the PLA/PEG blend (Ahmed, Mulla, & Arfat, 2016). Some other studies were carried out on the LLDPE-based films with the nanoparticle (Sanchez-Valdes, 2014). Unfortunately, no report is available on the combined effect of essential oil and bimetallic NPs on the LLDPE films and its characterization. In this study, the nanocomposite of LLDPE films was prepared by incorporating Ag-Cu NPs and CEO by compression molding and characterized those films by measuring their rheological, thermal and optical properties. Finally, the developed films were tested against *Salmonella* Typhimurium and *Campylobacter jejuni* using chicken meat as a model sample.

2. Materials and methods

2.1. Materials

A commercial grade LLDPE (EFDC-7087; Melt Index 1; density 0.92; Melting Point 124 °C) was procured from Equate Petrochemical Co. (Kuwait). Silver-copper alloy nanoparticles and cinnamon essential oil (CEO) were purchased from Sigma-Aldrich (St. Louis, MO, USA).

2.2. Bacterial strains and media

Culti-loops® of Gram-negative *Salmonella enterica sv* Typhimurium (ATCC 14028) and *Campylobacter jejuni* (ATCC 33291) was obtained from Remel Europe Limited (Dartford, Kent, UK) and Lyfo Disk pellets® of Gram-positive *Listeria monocytogenes* (ATCC 19114) strain was purchased from MediMark Europe (Grenoble, CEDEX, France). Tryptic soy broth (TSB) and Muller Hinton agar (MHA) were procured from TM Media (Bhiwadi, India). Brain heart infusion broth (BHIB) was obtained from Conda Laboratories (Torrejón de Ardoz, MD, Spain). Polymyxin-Acriflavin-Lithium chloride-Ceftazidime-Aesculin-Mannitol (PALCAM) agar base, Xylose lysine deoxycholate agar (XLD), PALCAM selective supplements, Campylobacter selective agar base, CampyGen™ gas generation sachet, Laked Horse Blood, Preston Campylobacter Selective Supplements and Campylobacter growth supplements were obtained from Oxoid (Basingstoke, HM, UK).

2.3. Preparation of compression molded LLDPE and composite films

(i) LLDPE/Ag-Cu (98/2 and 96/4) were compounded using a batch mixer Brabender® ATR Plasticorder (C.W. Brabender Instruments, Inc., South Hackensack, NJ, USA) equipped with 50 cm^3 mixing cell and torque recorder, at 180 °C, 80 rpm, for 5 min followed by compression molding with a thicknesses of 1 mm on a hot press (PHI QL438-C, City of Industry, CA, USA) at 172 °C by applying a force of 25 tons for 5 min, and finally cooled on a cold press to room temperature.

(ii) LLDPE and CEO blend at a ratio of 2:1 (50% CEO based on LLDPE w/w) were compounded using a twin-screw extruder (Century ZSK-30 (Century, Traverse City, MI, USA)) with a screw L/D ratio of 42, and a screw speed of 80 rpm. The temperature for the masterbatch preparation ranged between 160 and 180 °C in the different zones. Further, Ag-Cu and LLDPE/CEO master batch were mixed and compression molded in composite films (LLDPE/CEO/Ag-Cu 64/32/4) as described in step (i).

(iii) Neat LLDPE films were prepared by using the method described in step (i & ii) and used as a control.

2.4. Determination of film properties and characterization

2.4.1. Film thickness

Film thickness was measured by a digital micrometer (MCD-1″PXF, Mitutoyo Corp., Kawasaki-shi, Japan) with the sensitivity of 0.001 mm, at 10 random locations for each film.

2.4.2. Color, UV-barrier, light transmittance and transparency values

The color of the films was determined using a CIE colorimeter (Hunter associates laboratory, Inc., Reston, VA, USA), and expressed as L^* – (lightness), a^* – (redness/greenness) and b^*– (yellowness/blueness) values.

The light transmittance of films was measured at the ultraviolet and visible range (200 nm–800 nm) using a UV–visible spectrophotometer (Evolution 60s, Thermo Scientific, USA) according to the method of Ahmed, Hiremath, et al. (2016) and Ahmed, Mulla, et al. (2016). The transparency value of film was calculated using the following equation (Han & Floros, 1997):

$$\text{Transparency value} = \frac{-\log T_{600}}{x}$$

where T_{600} is the fractional transmittance at 600 nm and x is the film thickness (mm). The greater transparency value represents, the lower transparency of the film.

2.4.3. Rheological measurements

The melt rheology was performed on a Discovery Hybrid Rheometer HR-3 (TA Instruments, New Castle, DE, USA) equipped with an electrically heated plate (EHP). Film samples with the thickness of 0.5 mm were melted at selected temperatures (140, 150, 160 and 170 °C) for 5 min in the parallel plate fixture to eliminate residual stresses and then experienced various oscillatory measurements. Isothermal frequency sweeps (0.1–10 Hz) were performed in the linear regime, at a constant strain of 0.01% when the temperature had stabilized after loading the sample into the rheometer. All rheological measurements were carried out in duplicates, and rheological parameters were obtained directly from the computer software supplied by the manufacturer (TRIOS, TA Instruments, New Castle, DE, USA).

2.4.4. Barrier properties

The water vapor transmission rate (WVTR) was determined using Permatran W3/31 (Mocon, Inc., Minneapolis, MN, USA) according to ASTM standard F1249 (ASTM, 1995a). The nitrogen flow rate during the test was set at 100 cm^3/min. Samples were exposed to 50 ± 1% relative humidity (RH) and tested at 23 ± 1 °C. WVTR reached a steady state, usually after 6–8 h. The oxygen transmission rate (OTR) of films was measured at 23 °C and 50 ± 1% RH by an Extra-Solution Permeo$_2$ instrument (Capannori, LU, Italy) according to ASTM D3985-05 (ASTM, 1995b). Films with an open testing area of 50 cm^2 were placed into the test cell and exposed to 99% N_2 + 1% H_2 flow on one side and pure oxygen flow on the other. Gas flow was regulated at 20 mL/min. The water vapor and oxygen permeability values were

calculated by multiplying the respective transmission values by film thickness.

2.4.5. Thermal property measurement

Thermal analysis of LLDPE composite films (≈10 mg) was performed with a Q2000 differential scanning calorimeter (DSC) (TA Instruments, U.S.A.) under a nitrogen atmosphere. In the 1st cycle, samples were equilibrated at −60 °C and isothermed for 1 min; heated to 200 °C at 10 °C/min and isothermed for 1 min; cool to −60 °C at 10 °C/min and isothermed for 1 min. All steps were repeated in the 2nd cycle. The melting temperature (T_m), the crystallization temperature (T_c), the enthalpy and degree of crystallinity was determined from the instrumental software. Thermal scans for each sample were carried out in triplicate, and the average values are reported.

2.4.6. Attenuated total reflectance-fourier transform infrared (ATR-FTIR) spectroscopy

The FTIR analysis was performed on a Nicolet iS5 FTIR Spectrometer (Thermo Scientific, Madison, WI, USA). A total of 32 scans were accumulated in absorption mode with a resolution of 4 cm^{-1}. The spectrum was obtained from a range of 4000 to 550 cm^{-1}.

2.4.7. X-ray diffraction (XRD) analysis

XRD analysis of the selected films was performed on a Bruker D8 Advance diffractometer (Bruker AXS, Germany) equipped with Cu-Kα radiation (λ = 0.154 nm) at 40 kV and 250 mA. All samples were analyzed in continuous scan mode with the 2θ ranging from 5 to 80°.

2.4.8. Morphology

Surface morphology observations of film samples were performed in a JCM-6000 Plus, scanning electron microscope (SEM) (JEOL, Japan) at an accelerating voltage of 15 kV.

2.4.9. Effectiveness of films and assessing antibacterial properties

The antimicrobial effectiveness of the LLDPE, LLDPE/Ag-Cu, and LLDPE/Ag-Cu/CEO films was assessed against *S.* Typhimurium (Gram-negative), *C. jejuni* (Gram-negative) and *L. monocytogenes* (Gram-positive) using the liquid culture test (Ahmed, Hiremath, & Jacob, 2016; Ahmed, Hiremath, et al., 2016). The neat LLDPE film served as control.

2.4.10. Confirmation test with chicken

The antimicrobial effectiveness of LLDPE and LLDPE/Ag-Cu/CEO films against selected test organisms namely, *S.* Typhimurium, *C. jejuni,* and *L. monocytogenes* was tested on chicken meat as a model food system following our earlier work (Ahmed, Hiremath, et al., 2016). The sterilized chicken meat samples were randomly divided into two sets (10 g each set) for different bacteria inoculations. For inoculation of bacteria on chicken, a five mL aliquot of each organism strain (*S.* Typhimurium, *C. jejuni,* and *L. monocytogenes)* with a concentration of 1×10^8 CFU/mL inoculum was transferred onto the meat surface and spread evenly. Samples were left under a laminar hood for 30 min so that the inoculums attach onto the chicken after soaking. Afterward, minced chicken (about 1 g) contaminated with *L. monocytogenes or C. jejuni* or *S.* Typhimurium were wrapped individually with LLDPE and LLDPE/Ag-Cu/CEO films (5 × 5 cm), heat sealed and stored at 4 °C. Wrapped samples were collected and tested for the survival of test organisms by counting at different time intervals (0, 7, 14 and 21 days) during the storage. Chicken samples wrapped in the neat LLDPE films were considered as a control sample.

For determination, the number of bacterial growth on the sample, two packages for each test organism were used. The films were removed from the chicken sample, and the test organisms (*S.* Typhimurium and *L. monocytogenes)* on chicken were extracted in 10 mL of sterile buffered peptone water (0.1% w/v); homogenized in a vortex for 2 min. The same step was followed in 10 mL of sterile BHIB (0.1% w/v) to extract *C. jejuni* from the chicken sample. From the homogenate, serial dilutions were made in peptone water (*S.* Typhimurium or *L. monocytogenes*) and BHIB (*C. jejuni*); spread-plated on PALCAM agar for *L. monocytogenes,* XLD agar for *S.* Typhimurium and Campylobacter agar plates for *C. jejuni*, respectively. Plates were incubated at 37 °C for 48 h (*L. monocytogenes*), 37 °C for 24 h (*S.* Typhimurium) and 42 °C for 48 h under microaerophilic conditions (*C. jejuni*), the number of colonies formed was counted and reported as log CFU/g. All tests were evaluated in duplicate and repeated twice (n = 4).

2.5. Statistical analysis

All experiments were run in triplicate using three different lots of samples. Data were subjected to analysis of variance (ANOVA). Comparison of means was carried out by Duncan's multiple range tests (Steel & Torrie, 1980). Statistical analysis was performed using the Statistical Package for Social Science (SPSS 17.0 for Windows, SPSS Inc., Chicago, IL, U.S.A.).

3. Results and discussion

3.1. Thickness

The thickness of neat LLDPE and compression molded composites films is shown in Table 1. The thickness of the LLDPE films increased with the incorporation of Ag-Cu NPs and CEO, which is believed to be due to increase in solid contents. A similar increase in thickness was reported by Arfat, Ahmed, Hiremath, Auras, and Joseph (2017) for gelatin-based composite films.

3.2. Color, UV-barrier, light transmittance and transparency values

The surface color values of compression molded LLDPE films loaded with Ag-Cu NPs and CEO are shown in Table 1. The loading of NPs and CEO significantly affected the color values of LLDPE films ($P < 0.05$). The neat LLDPE film was transparent with L^* value of 92.12, which dropped significantly to 35.91 for LLDPE/4% Ag-Cu/50% CEO films ($P < 0.05$). On the contrary, a* and b* values increased with the loading of NPs and CEO, which indicated an increase in redness and yellowness in the nanocomposite film. Such transition in the color values was largely ascribed to the characteristic surface plasmon resonance (SPR) of Ag-Cu NPs and the coloring and phenolic components of the CEO.

The control LLDPE film exhibited poor light barrier property in the UV range (280 and 350 nm), and reinforcement of NPs decreased the transmittance significantly ($P < 0.05$) (Table 1), which can be attributed to the absorbance of UV light and the light scattering by the NPs dispersed in the film matrix. A similar observation was made for fish skin gelatin/Ag-Cu films (Arfat et al., 2017). The control LLDPE film had the lowest transparency value indicating the higher film transparency, which diminished with the incorporation of NPs and CEO ($P < 0.05$) because of the intense color attributed by NPs and CEO. Qin, Li, Liu, Yuan, and Li (2017) reported a similar lowering of transparency while incorporating various EOs into polylactic acid-based films. Bruna, Peñaloza, Guarda, Rodríguez, and Galotto (2012) observed an increase in opacity for MMT/Cu^{2+}/LDPE nanocomposites and stated that during the extrusion process copper gets interpolated into the clay mineral and thermally oxidized to copper

Table 1
Thickness, color, light transmittance and transparency values of compression molded LLDPE films loaded with Ag-Cu NPs and CEO.

Film sample	*Thickness (mm)	Color parameters										Transparency value
		L*	a*	b*	ΔE*							
		Light transmittance (%)										
		200	280	350	400	500	600	700	800			
Control LLDPE	0.096 ± 0.003^{c}	92.12 ± 0.06^{a}	−1.48 ± 0.003^{d}			−0.17 ± 0.015^{d}			1.57 ± 0.06^{d}			
LLDPE/2% Ag-Cu	0.098 ± 0.002^{c}	38.60 ± 0.005^{b}	0.65 ± 0.005^{c}			8.60 ± 0.165^{c}			55.77 ± 0.03^{c}			
LLDPE/4% Ag-Cu	0.103 ± 0.002^{b}	36.87 ± 0.13^{c}	0.84 ± 0.015^{b}			10.98 ± 0.005^{b}			57.90 ± 0.12^{b}			
LLDPE/4% Ag-Cu/50% CEO	0.107 ± 0.001^{a}	35.91 ± 0.92^{d}	1.27 ± 0.12^{a}			11.95 ± 0.245^{a}			59.10 ± 0.18^{a}			
Control LLDPE	33.23 ± 0.65^{a}	79.76 ± 0.68^{a}	84.32 ± 0.43^{a}	85.95 ± 0.38^{a}	87.93 ± 0.23^{a}	88.88 ± 0.16^{a}	89.58 ± 0.16^{a}		90.08 ± 0.03^{a}	0.53 ± 0.06^{d}		
LLDPE/2%Ag-Cu	4.42 ± 0.04^{b}	5.67 ± 0.06^{b}	6.92 ± 0.07^{b}	7.70 ± 0.02^{b}	8.90 ± 0.03^{b}	10.40 ± 0.04^{b}	9.01 ± 0.04^{b}		10.20 ± 0.05^{b}	10.03 ± 0.14^{c}		
LLDPE/4%Ag-Cu	1.03 ± 0.06^{c}	3.42 ± 0.01^{c}	4.57 ± 0.01^{c}	5.03 ± 0.05^{c}	6.03 ± 0.09^{c}	7.13 ± 0.09^{c}	8.31 ± 0.01^{c}		9.46 ± 0.08^{c}	10.72 ± 0.21^{b}		
LLDPE/4% Ag-Cu/50% CEO	0.05 ± 0.01^{d}	0.33 ± 0.01^{d}	0.57 ± 0.07^{d}	0.78 ± 0.03^{d}	1.02 ± 0.03^{d}	4.96 ± 0.07^{d}	2.31 ± 0.08^{d}		2.86 ± 0.06^{d}	12.08 ± 0.25^{a}		

Values are given as mean ± SD (n = 3).
*Film thickness values are given as mean ± SD (n = 10).
Different superscript letters in the same column indicate significant differences ($P < 0.05$).

oxide, which affects the opacity of the composite.

3.3. Rheological properties of LLDPE and composite films

While investigating the time-dependency of LLDPE and nanocomposites at 160 °C (Fig. 1a), it was found that both the LLDPE and the LLDPE/Ag-Cu nanocomposites showed time-independency as the complex viscosity, η* did not change with time, whereas, CEO incorporation into the LLDPE/Ag-Cu imparted the time dependency with a marginal increase in the η* from 0.49 to 0.54 Pa.s. Essential oil incorporation significantly influenced the composite rheology by acting as a plasticizer/lubricant. Additionally, the EO evaporates during a longer storage period, and the resultant film became more rigid with a higher G′ value.

Frequency-sweep measurements were made for each nanocomposite at selected temperatures (140, 150, 160 and 170 °C). The addition of Ag-Cu into LLDPE reinforces the polymer matrix and can be considered as an additive for improving the mechanical properties. Overall, both G′ and G″ increased gradually with increasing frequency with a predominantly liquid-like behavior (G″ > G′). The frequency sweep runs for the Ag-Cu/LLDPE, and Ag-Cu/CEO/LLDPE composites at 140 °C are illustrated in Fig. 1b. A distinct gel point (cross-over of G′ and G″) was detected during frequency sweep test; the frequency of the neat LLDPE was 5 Hz, which shifted to a higher value of 7.94 and 6.31 Hz with incorporating a loading of 4% Ag-Cu and 4% Ag−Cu/50% CEO, respectively. The addition of Ag-Cu in the LLDPE matrix could produce interconnected structures Ag-Cu–LLDPE, which influence the rheological response of the sample. As the loading of Ag-Cu nanoparticles increased such interactions begin to dominate and eventually lead to percolation, i.e. to the formation of Ag-Cu–LLDPE network, corresponding to a shift of liquid-like to solid-like behavior. On the contrary, incorporation of CEO into LLDPE/Ag-Cu lowered both G′ and G″ because of the presence of the plasticization effect attributed to the CEO.

The dispersion of nanoparticles into LLDPE matrix is examined by a Cole-Cole plot of the rheological data correlating real (η′) and imaginary (η″) parts of η* (Kim, Cho, Choi, & Park, 2000; Joshi, , Butola, Simon, & Kukaleva, 2006). Fig. 1c illustrates a Cole-Cole plot for LLDPE/Ag-Cu and LLDPE/Ag-Cu/CEO at 160 °C. A smooth, semicircular shape of the plotted curves indicates good compatibility of Ag-Cu (2–4%) and Ag-Cu/CEO into LLDPE, that is, phase homogeneity in the melt. It is worth mentioning that the Cole-Cole plot is not an absolute technique to determine the miscibility of blends. Another approach Van Gurp-Palmen analysis (a plot between [δ (phase angle) vs |G*| (complex modulus)], was also employed to understand the miscibility of nanoparticles and CEO into LLDPE (data not shown), and it was found that nanoparticles dispersed well whereas CEO containing Ag-Cu showed a slight deviation from the miscibility. The deviation could be influenced by plasticization/lubrication of CEO. At low values of |G*|δ is nearly 80°, meaning that the samples were almost viscous, and the value drops significantly to 30° at higher values indicating the elastic behavior appeared in that range.

The time-temperature superposition (TTS) principle was employed by applying both frequency shift and temperature shift for all the LLDPE nanocomposite rheograms, at selected temperatures (140–170 °C). It was observed that the generated master curve adequately superimposed all those rheograms into a single curve. A typical log-log master curve plots of η* vs frequency for LLDPE/4%Ag-Cu is shown in Fig. 1d at the 150 °C reference temperature.

3.4. Water vapor and oxygen permeability

WVP and OP values of compression molded LLDPE and composite films are given in Table 2. The obtained values for the neat LLDPE are in good agreement with previous reports (Hwang, Kwon, & Lee, 2017).

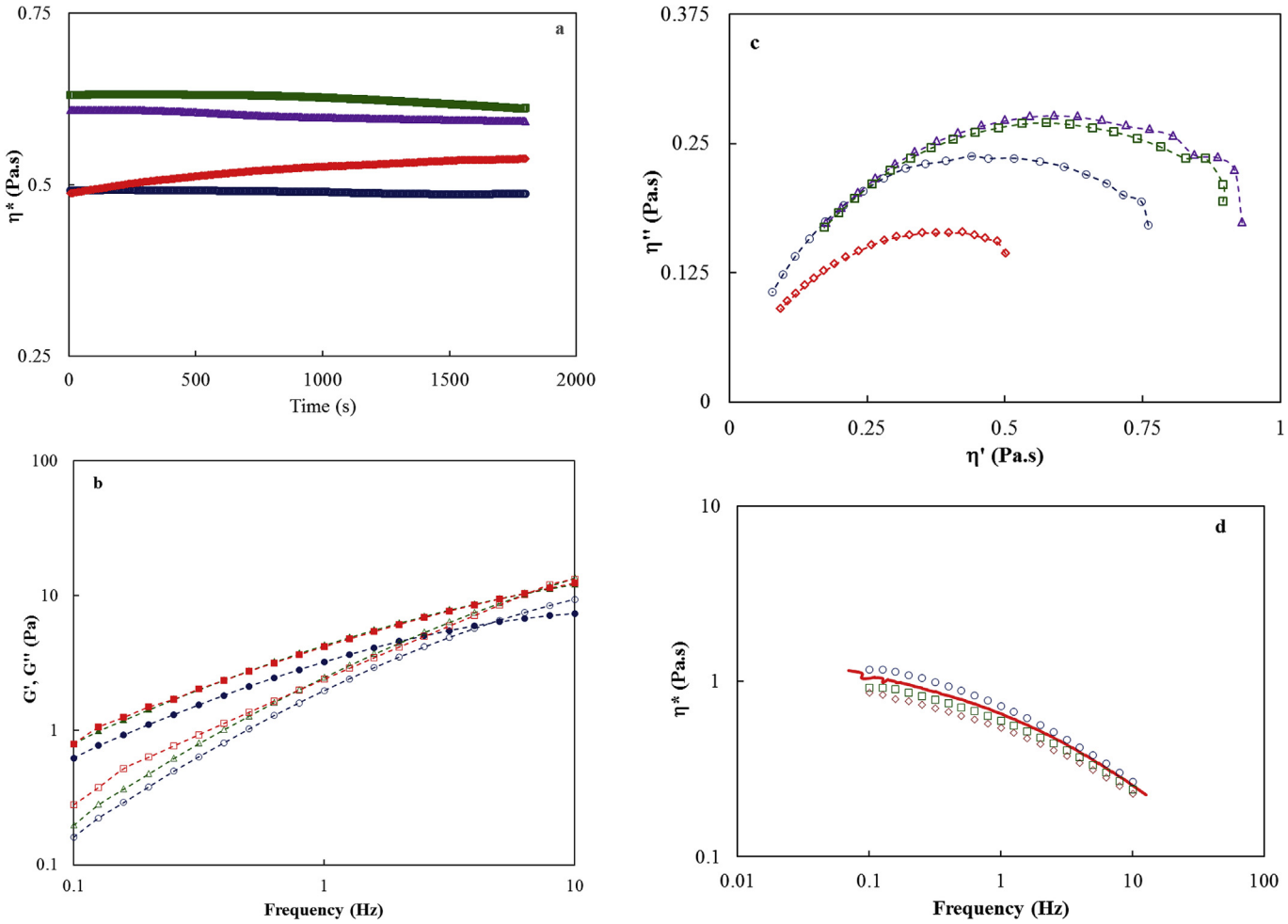

Fig. 1. Melt rheology of Ag-Cu and cinnamon essential oil incorporated LLDPE films (a) time dependency at 160 °C (◯–LLDPE, △–LLDPE + 2% Ag-Cu, □-LLDPE + 4% Ag-Cu and ◇-LLDPE + 4% Ag—Cu + 50% CEO), (b) rheograms of nanocomposites at 140 °C (◯–open and close G′ and G″ of LLDPE, △–open and close G′ and G″ of LLDPE + 4% Ag-Cu, □–open and close G′ and G″ of LLDPE + 4% Ag—Cu + 50% CEO), (c) Dispersion of nanoparticles ((◯–LLDPE, △–LLDPE + 2% Ag-Cu, □-LLDPE + 4% Ag-Cu and ◇-LLDPE + 4% Ag-Cu + 50% CEO), and (d) time-temperature superposition of 4% Ag-Cu doped LLDPE films (○ ◯ 140 °C, ━ MC at 150 °C, □–160 °C and ◇-170 °C).

Table 2
Water vapor and oxygen transmission rate of compression molded LLDPE films loaded with Ag-Cu NPs and CEO.

Film sample	Water vapor permeability (g mm/m^2 d atm)	Oxygen permeability (cc mm/m^2 d atm)
Control LLDPE	0.76 ± 0.04^a	109.14 ± 1.5^a
LLDPE/2% Ag-Cu	0.30 ± 0.02^c	89.07 ± 3.4^c
LLDPE/4% Ag-Cu	0.19 ± 0.03^d	74.88 ± 3.8^d
LLDPE/4% Ag-Cu/ 50% CEO	0.65 ± 0.01^b	102.85 ± 2.0^b

Values are given as mean ± SD (n = 3).
Different superscript letters in the same column indicates significant differences ($P < 0.05$).

WVP and OP values of LLDPE films decreased significantly ($P < 0.05$) after reinforcement of Ag-Cu NPs following the trend as reported earlier for silver nanoparticle deposited LLDPE/cyclo olefin copolymer blend films (Sanchez-Valdes, 2014). This behavior was attributed to the increase in a tortuous path, which causes interruptions in the diffusion of water vapor and oxygen from the LLDPE nanocomposite film. A reverse drastic increase in WVP and OP values was observed when 50% CEO was loaded into LLDPE/4% Ag-Cu polymer matrix. A similar trend was reported for films incorporated with basil essential oil (Bonilla, Vargas, Atarés, & Chiralt, 2011). The enormous increase in WVP and OP values could be occurred due to complex nature of CEO and its effect on cohesion forces with the polymer matrix.

Table 3
Thermal properties of compression molded LLDPE films loaded with Ag—Cu NPs and CEO.

Film sample	T_m/°C	ΔH_m/J.g^{-1}	T_c/°C	ΔH_c/Jg^{-1}	X_c/%
Control LLDPE	121.0 ± 0.0^c	75.4 ± 0.5^b	111.6 ± 0.1^b	37.2 ± 0.2^d	12.99 ± 0.6^d
LLDPE/2% Ag-Cu	122.0 ± 0.5^b	100.3 ± 0.3^a	112.1 ± 0.2^a	53.0 ± 0.3^c	18.4 ± 0.1^c
LLDPE/4% Ag-Cu	122.8 ± 0.2^a	101.0 ± 0.4^a	112.1 ± 0.0^a	87.1 ± 0.0^a	30.2 ± 0.3^a
LLDPE/4% Ag-Cu/50% CEO	120.2 ± 0.2^d	58.5 ± 4.0^c	108.2 ± 0.2^c	56.4 ± 1.2^b	20.2 ± 0.3^b

Values are given as mean ± SD (n = 3).
Different superscript letters in the same column indicate significant differences ($P < 0.05$).

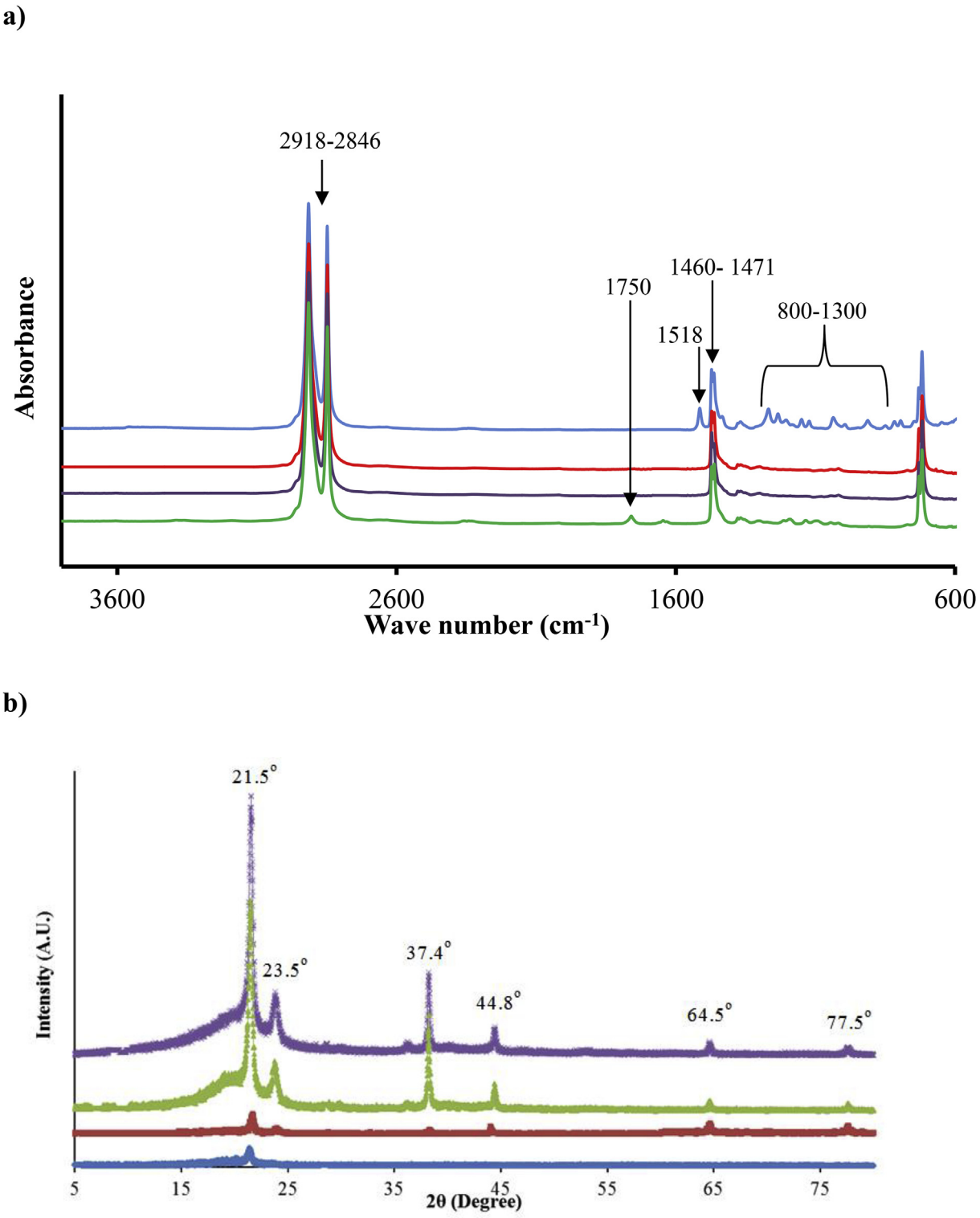

Fig. 2. a) FTIR spectra (LLDPE/4% A-Cu/50%CEO; LLDPE/4% Ag-Cu; LLDPE/2% Ag-Cu, and LLDPE) and b) XRD (LLDPE/4% Ag-Cu/50%CEO; LLDPE/4% Ag-Cu; LLDPE/2% Ag-Cu, and LLDPE) patterns of compression molded control LLDPE and LLDPE films incorporated with Ag-Cu NPs and CEO.

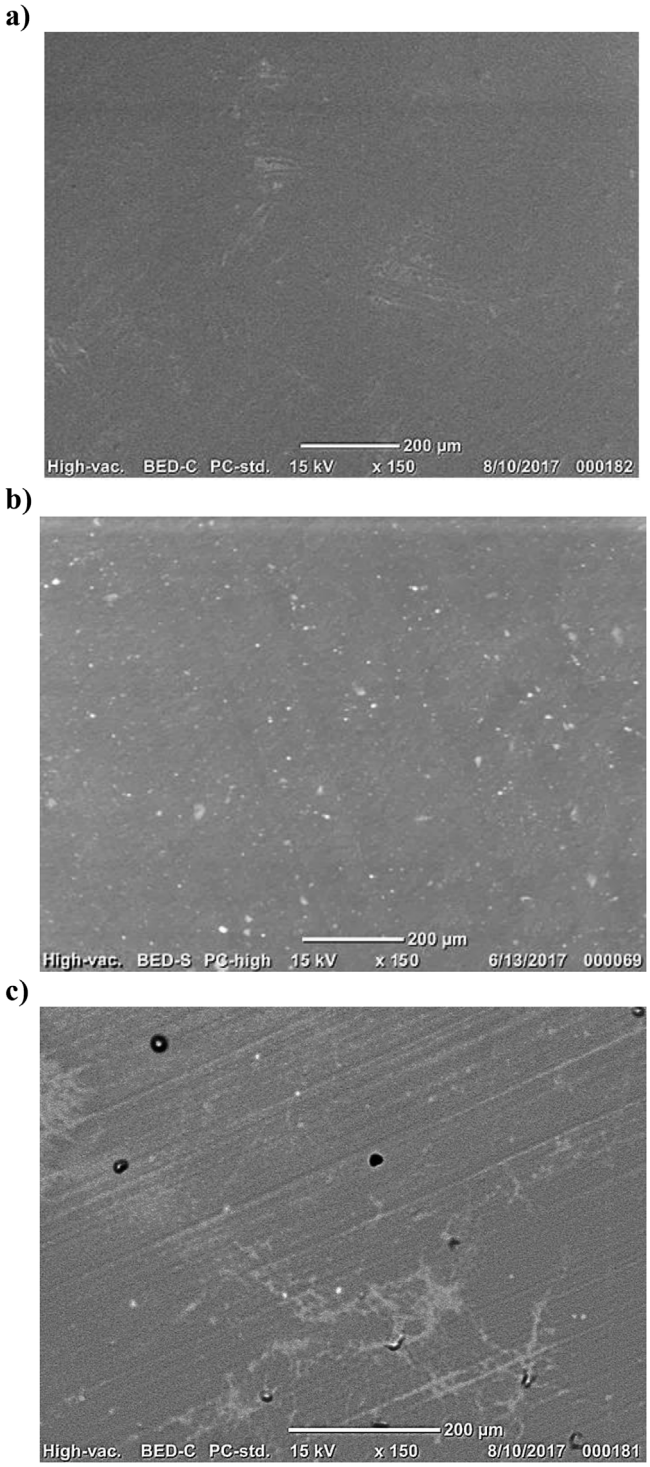

Fig. 3. Scanning surface electron micrographs of compression molded LLDPE films incorporated with bimetallic Ag-Cu NPs and CEO. Magnification: × 150. a) Control LLDPE film, b) LLDPE/4% Ag-Cu film and c) LLDPE/4% Ag-Cu/50% CEO film.

3.5. Thermal analysis

The T_m and T_c of the neat LLDPE films were about 121 and 111 °C, and the corresponding enthalpy (ΔH) values were 75.4 and 37.2 J/g, respectively (Table 3). As expected, the reinforcement of nanoparticles to the LLDPE matrix improved the T_m, T_c, ΔH and crystallinity (%X) significantly ($P < 0.05$), and those values equaled to 122.8°C, 112.1°C, 87.1 J/g, and 30.2% with a loading concentration of 4% (Table 3). A similar trend in enthalpy was observed for LLDPE/SiO_2 composite films containing SiO_2 (Kontou & Niaounakis, 2006).

The T_m, T_c, and %X values were significantly influenced by CEO incorporation, and the value dropped to 120.2, 108.2 °C and 20.2% at 50% CEO loading into LLDPE/4% Ag-Cu film ($P < 0.05$). The loading of EOs into LLDPE films improved the chain flexibility and reorganization of the low molecular weight polymer chains, resulting in reduced a T_m and T_c due to the plasticizing effect of the active compound (Medeiros, Ferreira, & Carciofi, 2017). The plasticization effect of CEO was further confirmed by rheological properties of the composite films as discussed earlier. A similar decreasing behavior in thermal properties of EOs loaded composite films has been reported (Ahmed, Hiremath, et al., 2016; Qin et al., 2017).

3.6. FTIR spectroscopy

Control LLDPE film represented the characteristic peaks at 2918-2846 cm^{-1} (CH_2 stretching), 1750 cm^{-1} (C=O stretching), 1460-1471 cm^{-1} (CH_2 bending), 1367 cm^{-1} (CH_3 bending) and 720-733 cm^{-1} (CH rocking) (Fig. 2a), and results are good in agreement with the published data (Wang et al., 2011). Most of the LLDPE peaks retained in the nanocomposite films except the peak at 1750 cm^{-1} (C=O stretching), which provides clear evidence that a chemical interaction has taken place between LLDPE and Ag-Cu NPs in the polymer matrix (Yang et al., 2010). LLDPE/4% Ag-Cu/50% CEO composite film exhibited an additional absorption peak at 1518 cm^{-1} (representing aromatic domain with NH bending) (Fig. 2a) and multitude of smaller bands in the region of 1300–800 cm^{-1}, which could be associated with the bending of the aromatic ring C—H bonds (Wen et al., 2016), and also confirmed an interaction of CEO with the polymer matrix.

3.7. X-ray diffraction (XRD) analysis

Two amorphous peaks at 21.5° and 23.5° were observed in the tested films, which characterize 110 and 200 lattice planes of the orthorhombic phase of polyethylene (Fig. 2b) as reported (Medjdoub, Guessoum, & Fois, 2017). However, the LLDPE films reinforced with Ag-Cu NPs revealed distinctive diffraction peaks at 37.4°, 44.8°, 64.5°, and 77.5° corresponding to the (111), (200), (220), and (311) planes of silver-copper nanoparticles (Fig. 2b) (Arfat et al., 2017; Tiimob et al., 2017). LLDPE/4% Ag-Cu/50% CEO films did not result in any change in XRD patterns, which is contrary to the reported data on LLDPE/MMT/EO (Efrati et al., 2014).

3.8. Microstructure

The SEM micrographs revealed that the smooth surface of control LLDPE film as compared to LLDPE composite films indicating the development of homogeneous and compact film structure (Fig. 3a). The surface of LLDPE loaded with 4% Ag-Cu NPs became coarse and showed well-dispersed bright dots (i.e., NPs) embedded in the film matrix. The coarseness was due to the distribution of NPs throughout the film matrix. The appearance of cracks on the LLDPE/Ag-Cu/CEO film surface revealed a poor distribution of particles and evaporation of CEO from the polymer matrix during the film processing and storage. Our observations are in good agreement with the results of Qin et al. (2017), who reported that EO droplets embedded in the film matrix result in the discontinuous film structure.

3.9. Antimicrobial activity of LLDPE and composite films

The *in-vitro* antimicrobial efficacy of LLDPE and composite films against *S.* Typhimurium, *L. monocytogenes*, and *C. jejuni* are illustrated in Fig. 4. The mean initial microbial counts of *S.* Typhimurium, *L. monocytogenes* and *C. jejuni* were 9.0, 9.3 and 7.3 log CFU/g, respectively. As expected, no antibacterial activity was detected for the neat

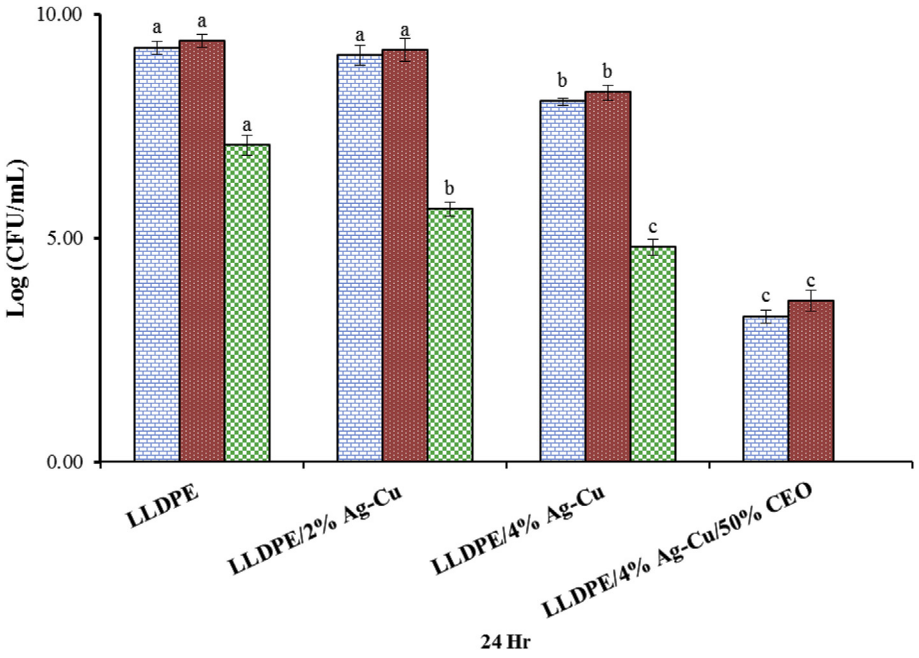

Fig. 4. *In vitro* antibacterial activities of compression molded LLDPE films incorporated with Ag-Cu NPs and CEO against *C. jejuni*, *S.* Typhimurium and *L. monocytogenes* after incubation for 24 h.

LLDPE film after 24 h of incubation whereas, the film containing 2% NPs showed a significant reduction of *C. jejuni* ($P < 0.05$). However, films containing 4% Ag-Cu NPs with or without CEO showed a marked effect against all tested microorganisms. The CEO incorporated films exhibited a complete inhibition against *C. jejuni*. The strong antibacterial activity and mechanisms of action of Ag-Cu NPs and CEO against the microorganisms have been demonstrated (Arfat et al., 2017; Burt, 2004). The mechanisms of inhibition of bimetallic Ag-Cu NPs against test microorganisms could be associated with the release of bimetallic nanoparticles that could penetrate into gaps and pits in the bacterial membrane, interact with sulfhydryl or disulfide groups of enzymes and other vital cell components, which finally lead to cellular death (Taner, Sayar, Yulug, & Suzer, 2011). Furthermore, cinnamaldehyde - the main compound present in the CEO can alter bacterial cell wall permeability, affect the enzyme activity and promote protein denaturation thereby leading to cell death (Sanla-Ead, Jangchud, Chonhenchob, & Suppakul, 2012).

3.10. Microbial validation of the film with chicken sample

Fig. 5 illustrates the growth of *S.* Typhimurium, *L. monocytogenes* and *C. jejuni* on artificially contaminated minced chicken packed in LLDPE and composite films under refrigerated storage for 21 days. The mean initial microbial counts of *S.* Typhimurium, *L. monocytogenes* and *C. jejuni* in inoculated chicken samples were 5.58, 8.63 and 5.32 log CFU/g, respectively. A significant reduction in bacterial counts was recorded on day 7, and it continued until day 21 for the chicken sample packed in LLDPE composite film ($P < 0.05$). The counts of *C. jejuni S.* and *S.* Typhimurium in chicken sample packed in LLDPE/4% Ag-Cu/50% CEO reached below the detection level on 7th and 14th day respectively. The observed data differed from our earlier work on packaging of chicken in PLA/PEG/CEO films, where, the counts of *S.* Typhimurium and *L. monocytogenes* chicken packaged in PLA/PEG film with 50% CEO reached below the detection level at 21 days (Ahmed, Hiremath, et al., 2016). A significantly higher reduction of *S.* Typhimurium and *C. jejuni* counts in LLDPE/4% Ag-Cu/50% CEO could be influenced by the presence of both Ag-Cu NPs and CEO. The antimicrobial effectiveness exhibited by the Gram-negative organisms over Gram-positive bacteria could be happened because of the difference in membrane charge and cell wall thickness of the bacterial strains (Shankar, Jaiswal, Selvakannan, Ham, & Rhim, 2016). A similar inhibitory effect was reported for LDPE/ethylene vinyl acetate/EO films against mold and fungi in sliced tomatoes stored for 20 days (Wattananawinrat, Threepopnatkul, & Kulsetthanchalee, 2014).

4. Conclusions

The reinforcement of Ag-Cu NPs in LLDPE films improved the mechanical, thermal and barrier properties of LLDPE films. Color and transparency of LLDPE films were significantly influenced by both Ag-Cu NPs and CEO ($P < 0.05$). The loading of CEO in LLDPE films improved the flexibility and UV barrier property. FTIR spectra confirmed chemical interactions between LLDPE and Ag-Cu NPs in the polymer matrix. XRD analysis revealed that the reinforcement of Ag-Cu NPs changed the crystal structure of LLDPE film. LLDPE films loaded with Ag-Cu NPs and CEO showed excellent antimicrobial properties and successfully inhibited the growth of microorganisms in the chicken samples during 21 days of storage at 4 °C. The LLDPE/Ag-Cu/CEO composite film can be used as an active packaging film to protect the raw chicken meat from pathogenic bacteria and undesirable photochemical reactions induced by UV light. Although nanopackaging has many potential benefits, still the safety of nanomaterials and the cost of the packaging materials remain a challenge for the industry and consumers. Nanoparticles could affect the cells, produce oral toxicity, inflammation, and skin toxicity. A better understanding and mathematical models about nanoparticle diffusion through packaging materials need to be developed. Addition of essential oil may influence the flavor and sensory profile of the packaged chicken. Therefore, a critical evaluation of nanocomposite and the essential oil is important before its commercial implementation.

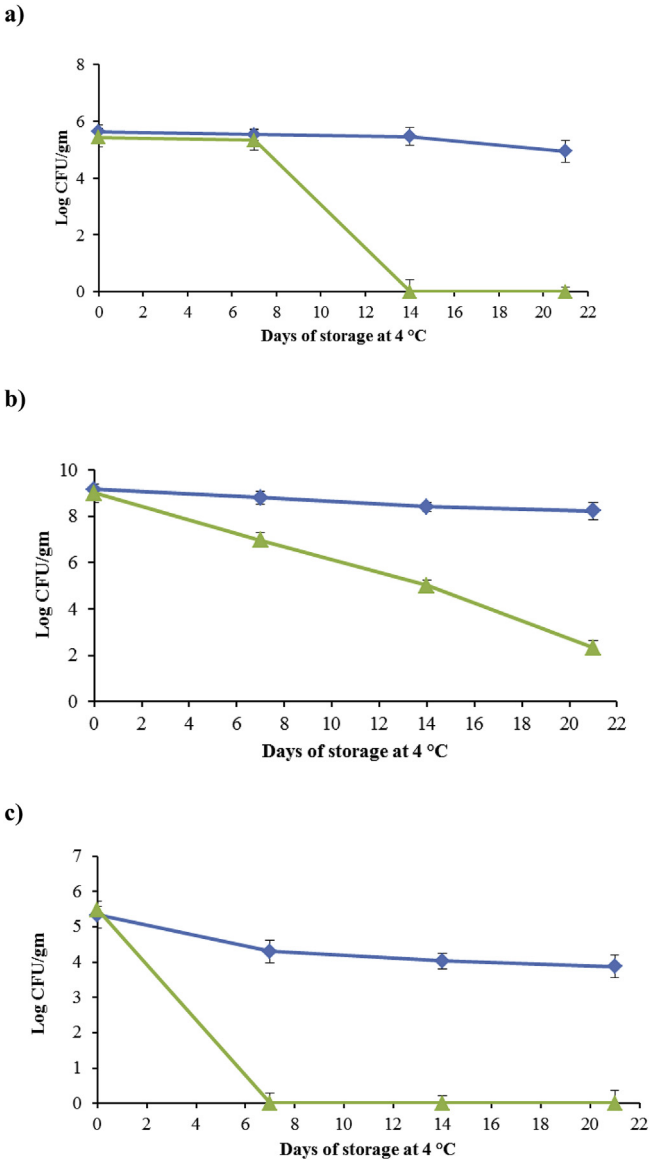

Fig. 5. Growth of *S.* Typhimurium, *L. monocytogenes* and *C. jejuni* in chicken meat samples wrapped with compression molded control LLDPE and LLDPE/4% Ag-Cu/50% CEO composite films and stored at 4 °C for 21 days (♦ LLDPE and ▲ LLDPE/4% Ag-Cu/50% CEO).

Acknowledgments

The author expresses their gratitude to the Kuwait Foundation for the Advancement of Science and Kuwait Institute for Scientific Research for providing the grant for the research work (Grant number FB087C).

References

Ahmed, J., Hiremath, N., & Jacob, H. (2016). Antimicrobial, rheological, and thermal properties of plasticized polylactide films incorporated with essential oils to inhibit *Staphylococcus aureus* and *Campylobacter jejuni*. *Journal of Food Science, 81*, 419–429.

Ahmed, J., Mulla, M. Z., & Arfat, Y. A. (2016). Thermo-mechanical, structural characterization and antibacterial performance of solvent casted polylactide/cinnamon oil composite films. *Food Control, 69*, 196–204.

Arfat, Y. A., Ahmed, J., Hiremath, N., Auras, R., & Joseph, A. (2017). Thermo-mechanical, rheological, structural and antimicrobial properties of bio-nanocomposite films based on fish skin gelatin and silver-copper nanoparticles. *Food Hydrocolloids, 62*, 191–202.

ASTM (1995a). Standard test method for water vapor transmission rate through plastic film and sheeting using a modulated infrared sensor. *Annual book of american standard testing methods, F1249*. Philadelphia, PA: ASTM.

ASTM (1995b). Standard test method for oxygen gas transmission rate through plastic film and sheeting using a coulometric sensor. *Annual book of american standard testing methods, D3985*. Philadelphia, PA: ASTM.

Berger, K., Keimel, C., Helfer, E., Haar, B., Mattausch, H., Riess, G., et al. (2017). The effects of e-beam crosslinking of LDPE on the permeation of hydrocarbons. *Journal of Applied Polymer Science, 134*, 44968. http://dx.doi.org/10.1002/app.44968.

Bonilla, J., Vargas, M., Atarés, L., & Chiralt, A. (2011). Physical properties of chitosan-basil essential oil edible films as affected by oil content and homogenization conditions. *Procedia Food Science, 1*, 50–56.

Bruna, J. E., Peñaloza, A., Guarda, A., Rodríguez, F., & Galotto, M. J. (2012). Development of MtCu $^{2+}$/LDPE nanocomposites with antimicrobial activity for potential use in food packaging. *Applied Clay Science, 58*, 79–87.

Burt, S. (2004). Essential oils: Their antibacterial properties and potential applications in foods—a review. *International Journal of Food Microbiology, 94*, 223–253.

Efrati, R., Natan, M., Pelah, A., Haberer, A., Banin, E., Dotan, A., et al. (2014). The combined effect of additives and processing on the thermal stability and controlled release of essential oils in antimicrobial films. *Journal of Applied Polymer Science, 131*, 40564. http://dx.doi.org/10.1002/app.40564.

EFSA (2009). *EFSA's 12th Scientific opinion on quantification of the risk posed by broiler meat to human Campylobacteriosis in the EU*. EFSA.

FDA (2015). Environmental decision memo for food contact notification No. 1569. Biologist, regulatory team 2. *Division of Biotechnology and GRAS notice review (HFS-255)*.

Han, J. H., & Floros, J. D. (1997). Casting antimicrobial packaging films and measuring their physical properties and antimicrobial activity. *Journal of Plastic Film and Sheeting, 13*, 287–298.

Hwang, K. S., Kwon, H. J., & Lee, J. Y. (2017). Water vapor permeability, morphological properties, and optical properties of variably hydrolyzed poly (vinyl alcohol)/linear low-density polyethylene composite films. *Korean Journal of Chemical Engineering, 34*, 539–546.

Joshi, M., Butola, B. S., Simon, G., & Kukaleva, N. (2006). Rheological and viscoelastic behavior of HDPE/octamethyl-POSS nanocomposites. *Macromolecules, 39*, 1839–1849.

Kim, C. H., Cho, K. Y., Choi, E. J., & Park, J. K. (2000). Effect of P (lLA-co-εCL) on the compatibility and crystallization behavior of PCL/PLLA blends. *Journal of Applied Polymer Science, 77*, 226–231.

Kontou, E., & Niaounakis, M. (2006). Thermo-mechanical properties of LLDPE/SiO_2 nanocomposites. *Polymer, 47*, 1267–1280.

Medeiros, G. R., Ferreira, S. R., & Carciofi, B. A. (2017). High-pressure carbon dioxide for impregnation of clove essential oil in LLDPE films. *Innovative Food Science & Emerging Technologies, 41*, 206–215.

Medjdoub, N., Guessoum, M., & Fois, M. (2017). Viscoelastic, thermal and environmental characteristics of poly (lactic acid), linear low-density polyethylene and low-density polyethylene ternary blends and composites. *Journal of Adhesion Science and Technology, 31*, 787–805.

Qin, Y., Li, W., Liu, D., Yuan, M., & Li, L. (2017). Development of active packaging film made from poly (lactic acid) incorporated essential oil. *Progress in Organic Coatings, 103*, 76–82.

Raquez, J. M., Habibi, Y., Murariu, M., & Dubois, P. (2013). Polylactide (PLA)-based nanocomposites. *Progress in Polymer Science, 38*, 1504–1542.

Rodriguez, A., Batlle, R., & Nerin, C. (2007). The use of natural essential oils as antimicrobial solutions in paper packaging. *Part II. Progress in Organic Coatings, 60*, 33–38.

Sanchez-Valdes, S. (2014). Sonochemical deposition of silver nanoparticles on linear low-density polyethylene/cyclo olefin copolymer blend films. *Polymer Bulletin, 71*, 1611–1624.

Sanla-Ead, N., Jangchud, A., Chonhenchob, V., & Suppakul, P. (2012). Antimicrobial Activity of cinnamaldehyde and eugenol and their activity after incorporation into cellulose-based packaging films. *Packaging Technology and Science, 25*, 7–17.

Scandorieiro, S., de Camargo, L. C., Lancheros, C. A., Yamada-Ogatta, S. F., Nakamura, C. V., de Oliveira, A. G., et al. (2016). Synergistic and additive effect of oregano essential oil and biological silver nanoparticles against multidrug-resistant bacterial strains. *Frontiers in Microbiology, 7*.

Shankar, S., Jaiswal, L., Selvakannan, P. R., Ham, K. S., & Rhim, J. W. (2016). Gelatin-based dissolvable antibacterial films reinforced with metallic nanoparticles. *RSC Advances, 6*, 67340–67352.

Steel, R. G. D., & Torrie, J. H. (1980). *Principle and procedure of statistics* (2nd ed.). New York: McGraw-Hill.

Taner, M., Sayar, N., Yulug, I. G., & Suzer, S. (2011). Synthesis, characterization and antibacterial investigation of silver-copper nanoalloys. *Journal of Materials Chemistry, 21*, 13150–13154.

Tiimob, B. J., Mwinyelle, G., Abdela, W., Samuel, T., Jeelani, S., & Rangari, V. K. (2017). Nano-engineered eggshell–silver tailored copolyester polymer blend film with antimicrobial properties. *Journal of Agricultural and Food Chemistry, 65*, 1967–1976.

Trimoulinard, A., Beral, M., Henry, I., Atiana, L., Porphyre, V., Tessier, C., et al. (2017). Contamination by *Salmonella* spp., *Campylobacter* spp. and *Listeria* spp. of most popular chicken-and pork-sausages sold in Reunion Island. *International Journal of Food Microbiology, 250*, 68–74.

Villaluenga, J. P. G., & Seoane, B. (1998). Influence of drawing on gas transport mechanism in LLDPE films. *Polymer, 39*, 3955–3965.

Wang, M., Wu, P., Sengupta, S. S., Chadhary, B. I., Cogen, J. M., & Li, B. (2011). Investigation of water diffusion in low-density polyethylene by attenuated total reflectance Fourier transform infrared spectroscopy and two-dimensional correlation analysis. *Industrial & Engineering Chemistry Research, 50*, 6447–6454.

Wattananawinrat, K., Threepopnatkul, P., & Kulsetthanchalee, C. (2014). Morphological and thermal properties of LDPE/EVA blended films and development of antimicrobial activity in food packaging film. *Energy Procedia, 56*, 1–9.

Wen, P., Zhu, D. H., Feng, K., Liu, F. J., Lou, W. Y., Li, N., et al. (2016). Fabrication of

electrospun polylactic acid nanofilm incorporating cinnamon essential oil/β-cyclodextrin inclusion complex for antimicrobial packaging. *Food Chemistry, 196*, 996–1004.

World Health Organization (2015). *WHO estimates of the global burden of foodborne diseases: Foodborne disease burden epidemiology reference group 2007-2015.* World Health Organization.

Yang, Z., Zhou, C., Cai, J., Yan, H., Huang, X., Yang, H., et al. (2010). Effects of macromolecular compatibilizers containing epoxy groups on the properties of linear low-density polyethylene/magnesium hydroxide composites. *Industrial & Engineering Chemistry Research, 49*, 6291–6301.

Zain, N. M., Stapley, A. G. F., & Shama, G. (2014). Green synthesis of silver and copper nanoparticles using Ascorbic acid and Chitosan for antimicrobial applications. *Carbohydrate Polymers, 112*, 195–202.